Selectivity of resonant Raman scattering in $InAs_xP_{1-x}$ solid solutions

E. Bedel, R. Carles, A. Zwick, J. B. Renucci, and M. A. Renucci
Laboratoire de Physique des Solides Associé au CNRS Université Paul Sabatier, 118 Route de Narbonne, 31062 Toulouse Cédex, France
(Received 9 April 1984)

The resonances of several structures (1LO, 2LO, disorder-activated TO, disorder-activated TA, disorder-activated LA, and local mode) in the Raman spectra of $InAs_xP_{1-x}$ alloys are investigated around the energy of the E_1 critical edge. Comparison with the resonances in mechanically perturbed InAs allows discrimination between the perturbations induced by either structural or chemical disorder inherent in the alloys. Large electron-phonon coupling for the longitudinal modes is seen, and the energy of the resonances is found to be dependent on the coherence length of the vibrational modes.

INTRODUCTION

Isoelectronic substitutions on either the anion or the cation site in a III-V compound induce two types of disorder. One, due to lattice relaxations in the vicinity of the foreign atoms, is referred as "structural." It destroys the translational symmetry and leads to a breakdown of the $\vec{q}=\vec{0}$ selection rule in a scattering process($\vec{q}$ is the pseudomomentum of the vibrational mode involved). This kind of disorder is already present in the pure compound when it is ion-implanted[1] or mechanically perturbed.[2] The other type of disorder, namely "chemical," induces, moreover, modifications in the masses and in the force constants between atoms, and thus affects the ionicity of the bonds.

The disorder affects both the vibronic and the electronic properties of the pure compound and, consequently, the electron-phonon interactions. Raman scattering allows one to investigate these different modifications.

The effects of disorder on the lattice dynamics have been studied extensively in the last few years using the Raman technique.[3–5] Indeed, the alteration of the frequency, symmetry, and broadening of the host-crystal modes provides information about the perturbation of the vibrational properties. Moreover, a new type of scattering interpreted as disorder-activated first-order Raman scattering (DAFORS) has been observed. It can lead, away from resonance, to an homogeneous activation of the one-phonon density of states.[6]

Resonant Raman scattering, on the other hand, allows one to study indirectly effects of disorder on electronic properties. In fact, the position and the width of the resonance curves reflect the perturbation incurred by the electronic states involved in the processes. Moreover, the theoretical interpretation of these curves allows one to discriminate easily between the various types of electron-phonon interactions.[7] Resonant Raman scattering has been investigated in several III-V mixed compounds, but always near the E_0 gap.[8,9]

In this paper we report on Raman scattering experiments in $InAs_xP_{1-x}$ solid solutions and analyze the resonance effects near the E_1 gap. The vibrational properties of this system have been presented elsewhere[10] and we shall add only few additional comments. We focus mainly on the resonance and try to discriminate between the modifications induced, whether by structural or chemical disorder.

The paper is organized as follows: Section I deals with vibronic properties, and the resonance is studied in Sec. II. All the samples used were epitaxial layers of n-type grown on InP(100) substrates.

I. VIBRATIONAL PROPERTIES

We first discuss the DAFORS and then explain the mode behavior of the structures.

A. Disorder-activated scattering.

In Fig. 1 we display the unanalyzed spectra, recorded at 300 and 77 K, for a concentration $x=0.70$. In the acoustical range (30–175 cm^{-1}) the intensities of the features at 90, 108, and 160 cm^{-1} decrease more rapidly with temperature than those located around 45–55 and 140–155 cm^{-1}. The former are well resolved in perfect InAs, and were attributed to overtones of acoustical phonons at L, X, and K, respectively;[10] consequently, the latter imply first-order processes. They were already assigned to transverse- (TA) and longitudinal-acoustic (LA) modes activated by the disorder, and labeled DATA (disorder-activated TA) and DALA (disorder-activated LA).[10]

In comparison with our previous work,[10] we note the clear resolution of the DATA band. Disorder-activated processes are now also apparent in the optical range. Indeed, for a (100) face only the LO(Γ) is allowed. Consequently, the large structure below the LO_2 peak in Fig. 1, named $DATO_2$, implies disorder-activated transverse-optical processes. Its narrowness originates from the weakness in the dispersion of the transverse-optical branches in InAs.[11] Similarly, the low-energy-side asymmetry of the LO_2 peak mirrors the longitudinal-optical—mode dispersion, and the shoulder is resolved at

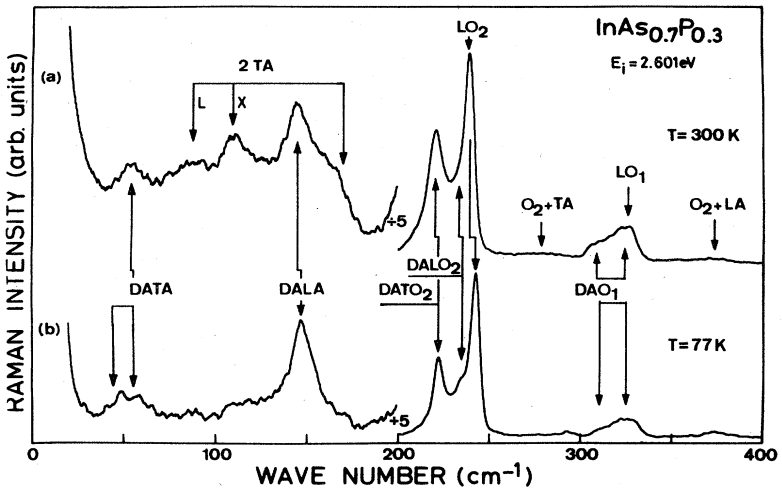

FIG. 1. Evolution with temperature of the low-frequency-range Raman spectra in $InAs_{0.7}P_{0.3}$. (a) $T=300$ K; (b) $T=77$ K.

77 K and named $DALO_2$ The DAO_1 scattering present in the InP-like band is also due to disorder. Its weakness originates from the small concentration of P and the very low Raman efficiency of InP.

The assignments presented above are confirmed by the polarization measurements displayed in Fig. 2. The spectra were recorded for three different experimental configurations in order to extract the three irreducible components Γ_1, Γ_{12}, and Γ_{15}. The exciting laser energy ($E_i=2.540$ eV) was chosen away from the E_1 resonance (see Sec. II). Within 10%, the allowed LO_2 peak has one Γ_{15} symmetry, as expected, whereas the $DATO_2$ and $DALO_2$ features possess both Γ_1 and Γ_{15} symmetry, demonstrating the different origin of these two scatterings. The peak at 320 cm^{-1} which merges into the local model $\omega_l(P{:}InAs)$ as x reaches 1, is also of Γ_{15} symmetry, as is found theoretically.[12] It is labeled O_1 in Fig. 2 since at that concentration the transverse or longitudinal character of the long-wavelength optical phonons of the InP band is already lost. The mixed symmetry (Γ_1 and Γ_{15}) of the DATA and the DALA features confirm similar results obtained for other III-V alloys.[13]

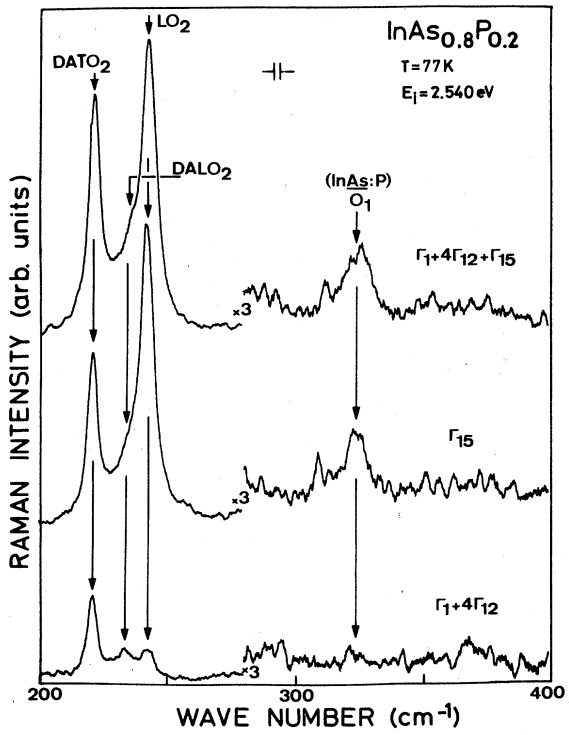

FIG. 2. Optical first-order selection rules observed at 77 K, out of resonance in $InAs_{0.8}P_{0.2}$. The scales are the same for the three configurations.

B. Mode behavior

As already shown,[10,14] $InAs_xP_{1-x}$ alloys follow two-mode behavior as long as long-wavelength optical phonons are involved. This mode behavior is related to the existence of two impurity modes: the local mode ($P{:}InAs$) and the gap mode ($As{:}InP$). The corresponding mode frequencies ω_l and ω_g are either determined experimentally or calculated. The theoretical calculations are always developed within a one-site model.[15] To calculate, for example, $\omega_l(P{:}InAs)$, one considers the perturbation of the dynamical matrix of InAs induced by a single embedded P atom. In order to reproduce the experimental localized-mode frequencies, large variations in the first-neighbor force constants are often needed[15]—this is physically questionable. Recently, a different model to calculate $\omega_l(P{:}InAs)$ was put forward,[16] in which one considers the perturbation induced on a tetrahedral unit of InP by changing the surrounding medium from InP to InAs. The local mode can then be viewed as the limit of the optical modes of InP which have progressively lost their identity (polarization, coherence length) with increasing InAs concentration. The "weighted" optical density of states merges in a δ function, the frequency of which

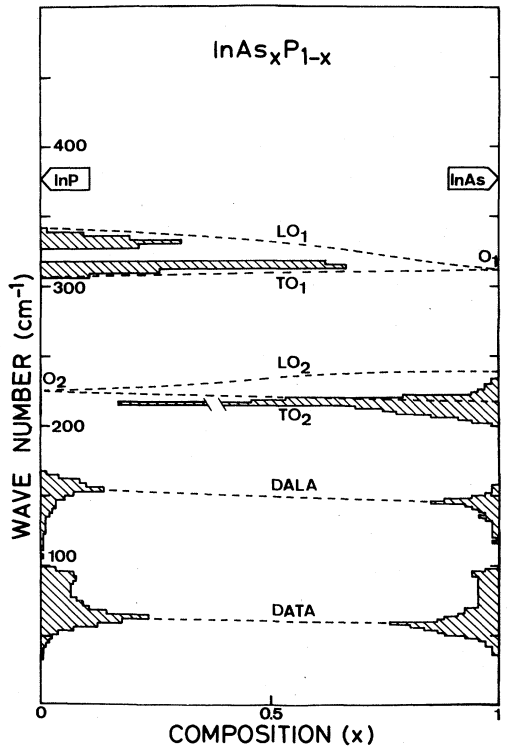

FIG. 3. Mode behavior of optical and acoustic modes in the $InAs_xP_{1-x}$ system. The one-phonon densities of states in InAs and InP are taken from Ref. 11. The dashed lines are least-squares fits to our previous experimental data (Ref. 10).

reproduces that of the localized mode.[16]

In Fig. 3 we show the calculated one-phonon densities of states of InAs and InP,[11] together with theoretical fits to the optical-phonon frequencies in the $InAs_xP_{1-x}$ system.[10] In any case, the frequencies of the optical densities-of-states maxima in InAs and InP are close to those of the gap and local modes, respectively. Within the model proposed, these frequencies are reproduced very well and explain the two-mode behavior of the $InAs_xP_{1-x}$ optical vibrations. The small variation of the TO_1 and TO_2 modes is also very understood since the transverse-optical branches in InAs and InP exhibit only a slight dispersion,[11] and the contribution of the modes to the weighted density of states is twice that of the longitudinal-optical modes. On the other hand, the large variation of the frequencies of the LO_1 and LO_2 modes is explained by reverse arguments.

The one-mode behavior of the TA and LA modes[10] also conforms to Jahne's criterion[17] since the transverse- and longitudinal-acoustical densities of states of InAs and InP, respectively, overlap (Fig. 3). Such behavior was already encountered in other III-V solid solutions.[13]

II. RESONANCE OF THE SPECTRA

In polar semiconductors two types of mechanisms are invoked to interpret the resonance phenomena.[7] One is the deformation-potential interaction, which is due to the modulation of the electronic susceptibility by the relative atomic displacements associated with a given mode. The other is the Frölich interaction, which concerns the coupling of the electrons with the macroscopic electric field which is attendant to a polar longitudinal mode. In the vicinity of the E_1 gap the allowed TO scattering includes both two- and three-band terms. For allowed LO scattering one must add the contribution due to the interband Frölich coupling. Forbidden LO scattering, important only near resonance, is explained by the Frölich intraband term, which is $\vec{q}$ dependent.

In this work, we study the resonance of the Raman spectra of several alloys ($x=0.40$, 0.70, and 0.80) near the E_1 edge. Nevertheless, we focus mainly on the concentration $x=0.80$ since it will be possible to discuss our results in the light of those already published for InAs.[18]

We present first, for that concentration, the symmetries near resonance of the optical bands, We then discuss, in detail, the resonances of the $1LO_2$, $2LO_2$, O_1, and O_1+LO_2 structures, and those of the disorder-activated bands (DATA, DALA, and $DATO_2$). Finally, we briefly comment on the spectra corresponding to other concentrations.

A. Symmetry near resonance

The conventional selection rules for allowed optical-phonon scattering are obtained by neglecting the $\vec{q}$ dependence of the modes.[19] Near resonance this assumption

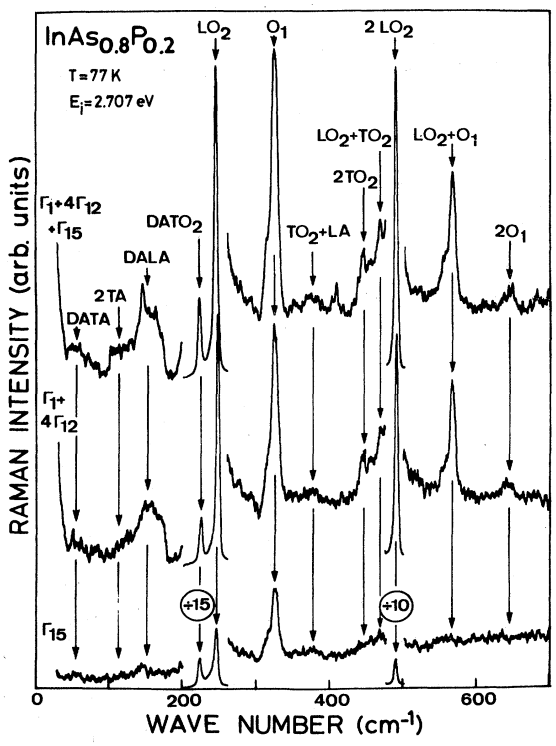

FIG. 4. Selection rules observed for $InAs_{0.08}P_{0.2}$ at 77 K in resonance conditions. The scales are the same for the three configurations.

TABLE I. Symmetries of the LO_2 $DATO_2$, O_1, and $2LO_2$ modes out of resonance, $E_i=2.409$ eV, and in resonance, $E_i=2.707$ eV.

Symmetry	$\frac{LO_2(\Gamma_1)}{LO_2(\Gamma_{15})}$	$\frac{DATO_2(\Gamma_1)}{DATO_2(\Gamma_{15})}$	$\frac{O_1(\Gamma_1)}{O_1(\Gamma_{15})}$	$\frac{2LO_2(\Gamma_1)}{2LO_2(\Gamma_{15})}$
$E_i=2.409$ eV	0.09	0.5	~0.2	
$E_i=2.707$ eV	4.4	1.6	2.6	8.65

breaks down and new selection rules are deduced for the corresponding forbidden scattering.[20] For the III-V compounds the LO- and TO-allowed scattering has Γ_{15} symmetry. For the forbidden intraband LO scattering it has been shown[21] that, near E_1, the strongest contribution is expected in a parallel-parallel configuration. Such a configuration always implies Γ_1 symmetry for the Raman tensor, and, consequently, the symmetry of those forbidden scattering is termed Γ_1-like.

In Fig. 4 we present Raman spectra recorded near resonance ($E_i=2.707$ eV). To show quantitatively how the symmetry is affected by resonance effects, in Table I we give the intensity ratio of the Γ_1 to Γ_{15} symmetry which enters a given structure near and out of resonance. In fact, the ratio $I(\Gamma_1)/I(\Gamma_{15})$ is reduced by a factor of 50 for the $1LO_2$ mode. This ratio, reduced by a factor of 13 for the local mode O_1, suggests Frölich coupling for this mode as well. The $2LO_2$ and LO_2+O_1 scattering, totally Γ_1 polarized, is only present at resonance, thus revealing the same type of coupling.

B. Resonances of the $1LO_2$ and $2LO_2$ modes

The forbidden LO-scattering resonance is well explained by the intraband term of the Frölich interaction[7] which gives rise to sharper enhancements than those involving the deformation-potential interaction. Indeed, near E_1 the Raman tensor is proportional to the second derivative versus energy of the electronic susceptibility.[21]

For that reason, the LO_2 and $2LO_2$ intensities have been normalized to that of the $DATO_2$, which is much less dispersive (see Sec. II D). This procedure, although somewhat rough, nevertheless allows one to avoid corrections for the ω^4 law, the optical properties of the sample, and the spectral response of the setup.[18]

In Fig. 5 we display the evolution, with exciting laser energy, of the spectra normalized in this way and recorded at 77 K. One first notices the high $2LO_2$-scattering efficiency, which is of the same order of magnitude as the LO_2 one near resonance. This has been observed already for several III-V alloys near the E_0 gap, and has led to the replica notion.[22,23] On the other hand, a small shift appears between the LO_2 resonances: the recorded intensity of the LO_2 resonance is maximum for $E_i=2.661$ eV, whereas the $2LO_2$ resonance reaches its highest value for $E_i=2.707$ eV. The LO_2 and $2LO_2$ widths are similar and comparable to those found in pure InAs.[18]

Out of resonance ($E_i=2.497$ eV) the LO_2 peak corresponds to allowed scattering, so we use the value of the ratio $I(LO_2)/I(DATO_2)$ out of resonance to remove the LO_2-allowed contribution. Consequently, the LO_2-normalized intensity plotted in Fig. 6 concerns only the forbidden contribution. In this figure we also display the $2LO_2$-normalized intensity versus incident-laser energy, and similar data obtained for perfect InAs.

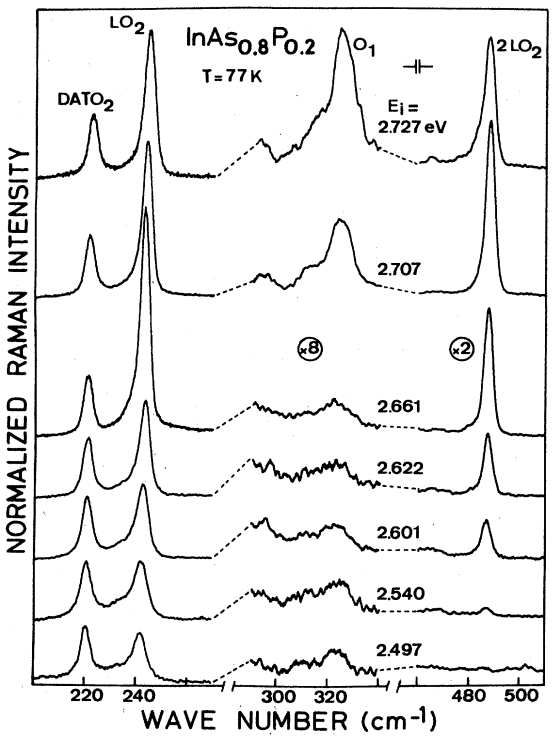

FIG. 5. Evolution with exciting laser energy (E_i), at 77 K, of the Raman spectra of $InAs_{0.8}P_{0.2}$ in the vicinity of the E_1 edge. These spectra are normalized to the $DATO_2$-scattering intensity.

These experimental points are fitted following the method explained in Ref. 21. We used the expression

$$I=\frac{H}{[(E_i-E_1)^2+\Delta^2]^2},$$

where E_1, Δ, and H are, respectively, the maximum, the half width, and the height of the resonance curve. These quantities were used as least-squares-fitted adjustable parameters.

The deduced theoretical curves are drawn in Fig. 6 and show very good agreement with the corresponding experimental data, which thus supports the hypothesis of intraband Frölich coupling. One notes the unexpectedly high value of the ratio of second- to first-order efficiencies in the alloy in contrast to that for the case of a pure compound. The small shift between the $1LO_2$ and $2LO_2$ resonances in the alloy is attributed to a double resonance at the incident- and scattered-photon energies.[9] This double resonance cannot be resolved since the widths of the resonances (≃90 meV) are much larger than the LO_2-phonon energy.

Away from resonance, it has been shown[10] that the Raman spectra of $InAs_xP_{1-x}$ alloys containing little phosphorus are similar to those of pure mechanically altered

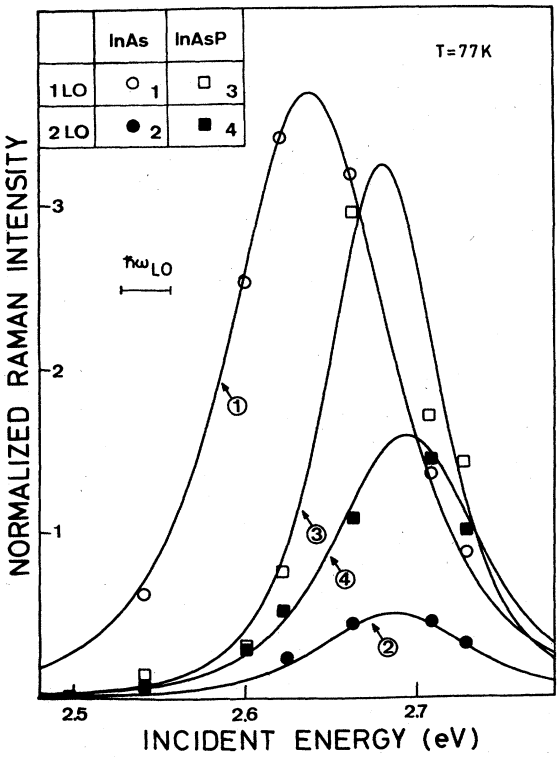

FIG. 6. Resonance of the forbidden 1LO and 2LO InAs-like modes in $InAS_{0.8}P_{0.2}$, and in pure InAs at 77 K. The solid lines correspond to theoretical fits (see text). All the intensities are normalized to the $DATO_2$ ($InAs_{0.8}P_{0.2}$) or the TO(Γ) intensities (InAs).

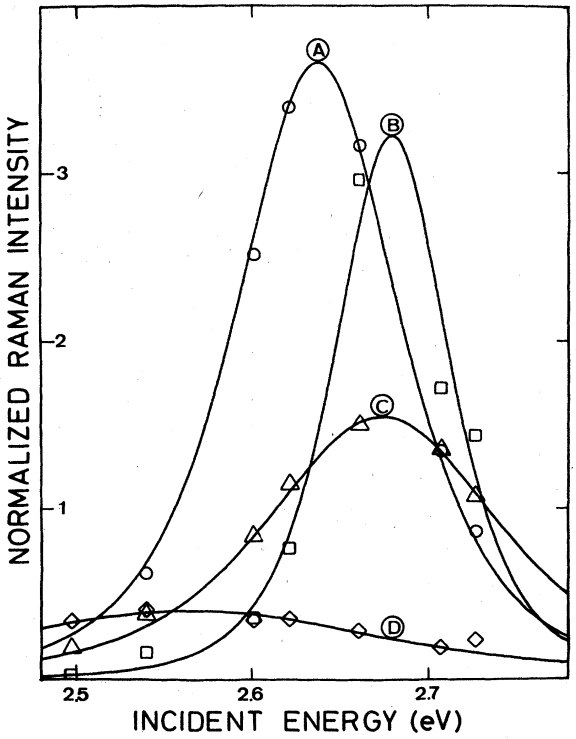

FIG. 7. Resonance Raman scattering for forbidden 1LO scattering in pure InAs at 77 K (A), in $InAs_{0.8}P_{0.2}$ at 77 K (B), and in mechanically altered InAs at 100 K (C) and 300 K (D). The solid lines correspond to theoretical fits (see text). All the intensities are normalized to the $DATO_2$ ($InAs_{0.8}P_{0.2}$) or the TO(Γ) intensities (InAs).

InAs. In the latter case the disorder present is only structural. In order to discriminate between structural- and chemical-disorder influences in the alloy near resonance, we show in Fig. 7 the low-temperature resonance curves of the $1LO_2$ resonance in $InAs_{0.80}P_{0.20}$ and mechanically altered InAs.[24] The resonance at 300 K is also shown, in the latter case, to illustrate the thermal disorder.

The parameters E_1, Δ, and H deduced from all these fits are listed in Table II together with the intensity of the resonances defined arbitrarily as $I=H\Delta$. Let us first comment on the variations of E_1 and Δ.

As already discussed, in perfect InAs (Ref. 18) the thermal disorder induces a shift to lower energy of the maximum E_1 ($C\rightarrow D$ in Fig. 7). The width Δ increases, indicating a shortening of the lifetime of the electronic states involved. For structural disorder ($A\rightarrow C$), the small increase of E_1, if significant, may be attributed to local strains going along with the mechanical perturbation. Such strains were invoked to explain the broadening of vibrational modes in such samples.[2] The main consequence of the structural disorder is a larger width Δ (a factor of 1.5 compared to perfect InAs; see Table II). Indeed, the electronic wave functions are more or less perturbed depending on the size of the microdomains created during the mechanical alteration of the sample. In contrast, no broadening is apparent when one goes from the pure compound to the alloy ($A\rightarrow B$). If we suppose that the selectivity of the LO coupling is the same, we can conclude that there is less structural-disorder influence in this case and that chemical-disorder influence on the coupling involved is small. As evidence of the long coherence length of the electronic and vibronic excitations implied, the shift of the resonance curve in the alloy reflects only the increase of the E_1 optical transition from InAs to InP.

We now turn to the intensity I of the resonance due, in part, to the strength of the electron-phonon coupling. The intensity I diminishes with thermal disorder. This effect is more evident for the $1LO_2$ resonance than for the $2LO_2$ resonance because of the greater influence of the population factor in the latter case. The decrease encountered for the chemical and the structural disorders ($A\rightarrow B$ and $A\rightarrow C$, respectively) is comparable for the $1LO_2$ scattering, in contrast to what happens for the $2LO_2$ case. Indeed, the $2LO_2$-resonance intensity is enhanced by more than a factor of 2 when compared to perfect InAs, whereas it decreases by a factor of 2 for perturbed InAs. Since the relaxation of the $\vec{q}=\vec{0}$ selection rule allows the participation of more phonons in the scattering processes, as emphasized in the lattice-dynamical behavior (Sec. I), the attenuation of the resonance by structural disorder implies the decrease of the coupling. In contrast, the enhancement of the resonance by chemical disorder implies a great strengthening of the coupling. (This

strengthening actually occurs since, near resonance, the widths of the LO peaks are not enlarged by the participation of $\vec{q}\neq\vec{0}$ phonons.) A nondirect $\vec{q}$ dependence of the forbidden Frölich mechanism has also been invoked in other experiments.[24]

The explanation of the enhancement of the LO resonance in the alloy could lie in the coupling of these modes with local fields arising from the potential fluctuations due to the impurity atoms. Such large couplings ($\vec{q}$ dependent) have been found when external fields are applied to semiconductors or when internal fields appear near the surfaces of accumulated or depleted samples.[25]

C. Resonances of the O_1 and O_1+LO_2 modes

In Fig. 5 the O_1-mode intensity has also been normalized to that of the $DATO_2$ one. One notes it is still increasing for $E_i=2.727$ eV, whereas the LO_2 and $2LO_2$ resonances are not. The corresponding data, together with those for the O_1+LO_2 resonance are plotted in Fig. 8. They show sharp enhancements as for the $1LO_2$ and $2LO_2$ intensities, but at much higher incident energy. Such a large observed shift (>60 meV) is out of the range of the usual shifts observed between different first-order resonance curves in the pure compound. In fact, the energy of the O_1-mode resonance would be nearer to the InP E_1 gap than that of the $InAs_{0.8}P_{0.2}$ one. As a consequence of the high degree of localization of the O_1 mode in the vicinity of the phosphorus atom, use of delocalized functions for the intermediate states entering the matrix elements of the electron-phonon interaction is irrelevant. This localization reinforces the InP-like character, and thus a molecular point of view is certainly more than adequate to describe this effect. Such couplings between localized vibrations and electronic levels associated with impurities have already been reported in the case of nonisoelectronic substitutions.[27,28]

D. Resonance of the DAFORS

In Fig. 9 we display the spectra of the disorder-activated bands (DATA, DALA, and $DATO_2$) recorded with four different exciting laser energies. They have been normalized only to the incident-laser power. This crude procedure cannot significantly affect the resonances since variations due to "correction factors" near the E_1 edge are not important.[18]

In the acoustical range one notes a selective enhancement of the longitudinal scattering. This is even more evident in Fig. 10 where the different resonances are plotted. Within experimental uncertainties the DATA cross section is not dispersive, whereas that of DALA clearly resonates around 2.66 eV. Selective enhancements have been reported recently in the $Ga_{1-x}Al_xAs$ system:[29,3] They concern both the transverse- and longitudinal-acoustic bands, whereas in the present system the selectivity favors only the longitudinal one. The DALA and the $DATO_2$ resonances are less sharp than those of the

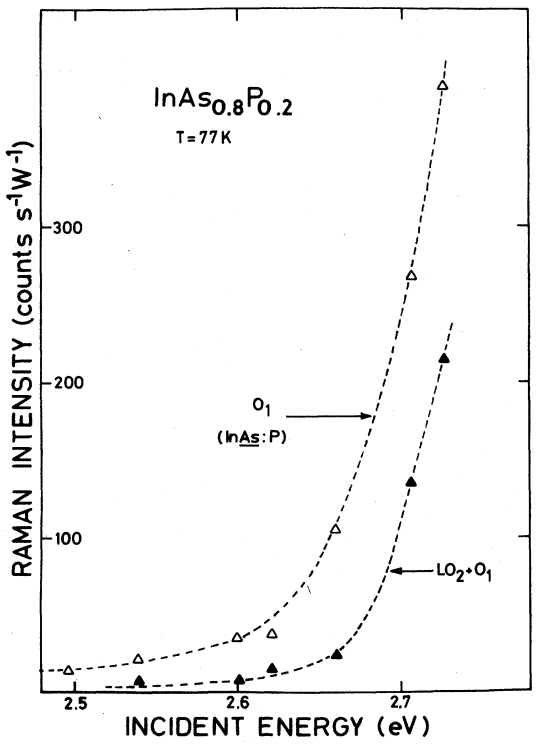

FIG. 8. Resonance of the O_1 local mode and its LO_2 replica in $InAs_{0.8}P_{0.2}$ at 77 K. The experimental data are only normalized to incident-power energy. The dashed lines are guides for the eyes.

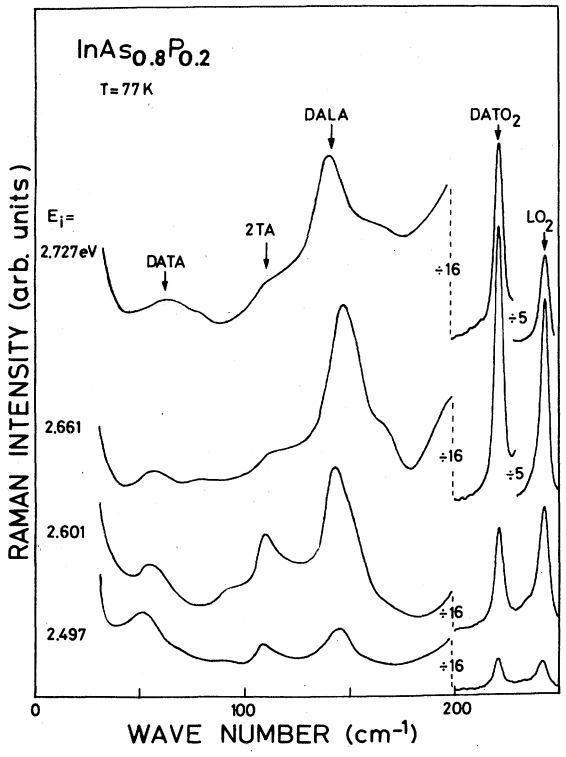

FIG. 9. Evolution with exciting laser energy (E_i), at 77 K, of the disorder-activated Raman bands in $InAs_{0.8}P_{0.2}$ in the vicinity of the E_1 edge. The spectra are normalized to incident-power energy.

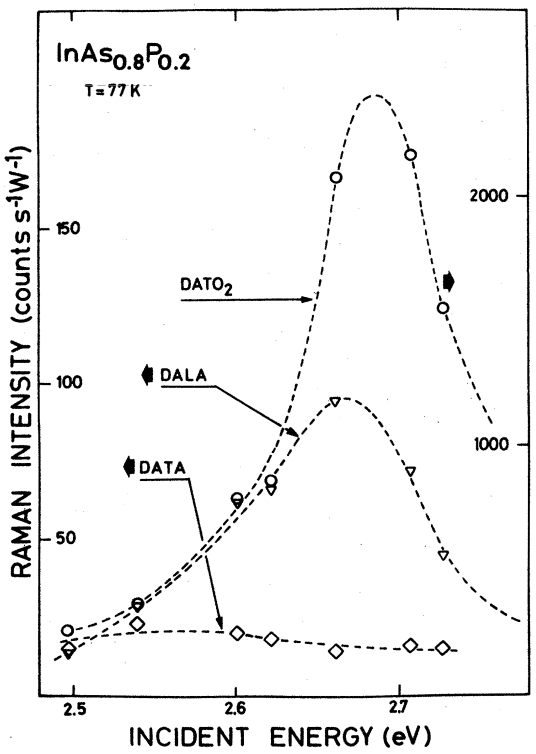

FIG. 10. Disorder-activated first-order resonances in $InAs_{0.8}P_{0.2}$ at 77 K. The experimental data are normalized to incident-power energy, and the dotted lines are guides for the eyes.

LO_2 and $2LO_2$, a result which supports the normalization procedure used to analyze the latter (see Sec. II B). They take place, nevertheless, at similar energies, revealing, in DAFORS as well, the rather long coherence length of the implied vibrational modes. The weak resonance of the DALA and the $DATO_2$ bands imply that the deformation-potential coupling is prominent although an electro-optic contribution cannot be ruled out. This is certainly true for the DALA modes as emphasized by the large value of the I(DALA)/I(DATA) ratio. For the $DATO_2$ scattering as well, this contribution can be significant since even in the perfect crystal the transverse nature of the modes implied is only valid for high-symmetry directions; in any case the polarization of these modes is progressively lost with increasing disorder. This could explain the value of the $I(\Gamma_1)/I(\Gamma_{15})$ ratio found at resonance for the $DATO_2$ case (see Table II).

TABLE II. Comparison of the $1LO_2$ and $2LO_2$ resonances. The intensities have been normalized to that of the $DATO_2$ ($InAS_{0.8}P_{0.2}$) or the TO(Γ) (InAs).

	Perfect InAs (77 K) (*A*)	$InAs_{0.8}P_{0.2}$ (77 K) (*B*)	Mechanically perturbed InAs (100 K) (*C*)	Mechanically perturbed InAs (300 K) (*D*)
		$1LO_2$ mode		
E_1 (eV)	2.638	2.680	2.674	2.566
Δ (meV)	56	41	88	136
H	3.68	3.27	1.56	0.42
$I=H\Delta$	206	134	137	57
		$2LO_2$ mode		
E_1 (eV)	2.683	2.693	2.699	2.586
Δ (meV)	56	49	82	110
H	0.51	1.58	0.21	0.09
$I=H\Delta$	29	77	17	10

E. Role of concentration

In Figs. 11 and 12 we display the spectra recorded near the E_1 resonance for two other concentrations, $x=0.70$ and 0.40. The assignments of the prominent features of

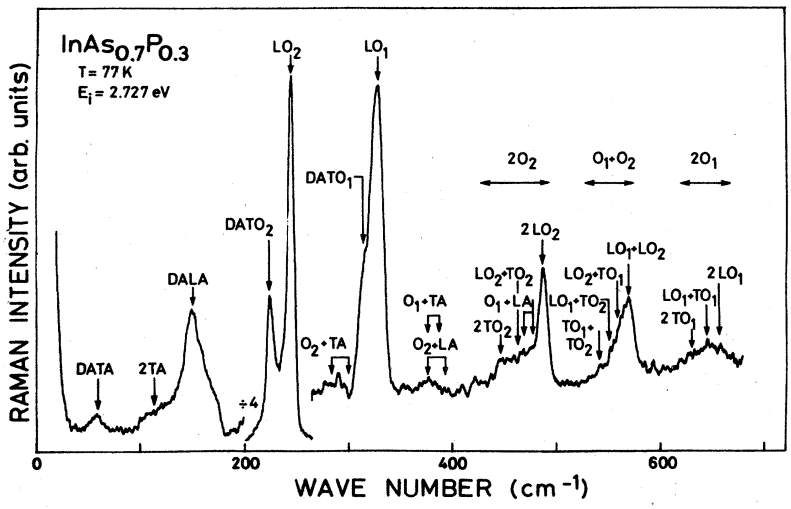

FIG. 11. Raman spectra for $InAs_{0.7}P_{0.3}$ at 77 K.

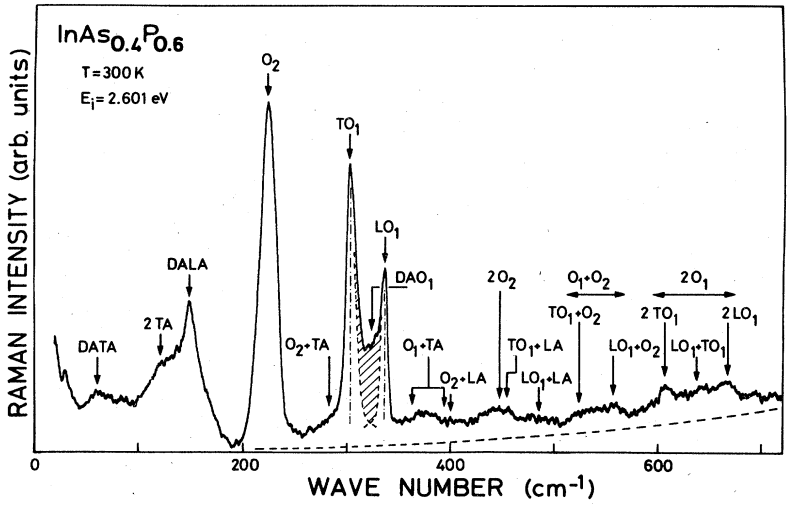

FIG. 12. Raman spectra for $InAs_{0.4}P_{0.6}$ at 300 K.

the spectra involve mainly the replicas of the LO_1 and LO_2 modes. Whereas the structural disorder of the alloy weakens the second-order features, the strength of the electron—longitudinal-mode coupling is not altered by an increase in chemical disorder.

CONCLUSION

Among the results presented we would like to first note the strong selective enhancements observed for the forbidden $1LO_2$ and $2LO_2$ modes at the E_1 gap, which we attribute to the strengthening of the electron-phonon coupling probably induced by the local electric field associated with potential fluctuations. The resonance of these long-coherence-length modes indicate an averaged band structure for the alloy. On the other hand, the O_1 local mode has a large resonance which reaches a maximum at a different exciting energy. The shift is explained by the short coherence length of this vibrational mode which is then coupled with the electrons. Indeed, the spatially well-localized O_1 mode selects only the part of the electronic wave functions around the foreign atom and thus emphasizes their InP-like character. In conclusion, resonant Raman scattering appears to be an efficient probe to test more or less localized electron-phonon interactions by choosing the appropriate vibrational mode to investigate.

ACKNOWLEDGMENTS

We are grateful to Dr. R. J. Nicholas for the loan of the $InAs_{1-x}P_x$ samples grown at the Royal Signals and Radar Establishment, Baldock, United Kingdom, by Dr. M. L. Yound. This work was supported by the Centre National d'Etudes des Telecommunications.

[1]S. Ushioda, Solid State Commun. **11**, 1127 (1972).
[2]D. J. Evans and S. Ushioda, Phys. Rev. B **9**, 1638 (1974).
[3]H. Kawamura, R. Kawamura, R. Tsu, and L. Esaki, Phys. Rev. Lett. **29**, 1397 (1972).
[4]B. Jusserand and J. Sapriel, Phys. Rev. B **24**, 7194 (1981); N. Saint-Cricq, R. Carles, J. B. Renucci, A. Zwick, and M. A. Renucci, Solid State Commun. **39**, 1137 (1981).
[5]B. Kh. Bairamov, V. N. Vishnevskü, M. I. Demchuk, V. V. Toporov, Sh. B. Ubaidullaev, L. Hildish, and E. Jahne, Fiz. Tverd Tela (Leningrad) **23**, 23 (1981) [Sov. Phys.—Solid State **23**, 13 (1981).
[6]R. Carles, A. Zwick, M. A. Renucci, and J. B. Renucci, Solid State Commun. **41**, 557 (1982).
[7]M. Cardona, in *Light Scattering in Solids II*, Vol. 50 of *Topics in Applied Physics*, edited by M. Cardona and G. Gunterhodt (Springer, Berlin, 1982), p. 19.
[8]J. Shah, A. E. DiGiovanni, T. C. Damen, and B. J. Miller, Phys. Rev. B **7**, 3481 (1973).
[9]M. Oueslati, C. Hirlimann, and M. Balkanski, J. Phys. (Paris) **42**, 1151 (1981).
[10]R. Carles, N. Saint-Cricq, J. B. Renucci, and R. J. Nicholas, J. Phys. C **13**, 899 (1980).
[11]P. H. Borcherds and K. Kunc, J. Phys. C **11**, 4145 (1978).
[12]R. Loudon, Proc. R. Soc. London **84**, 379 (1964).
[13]R. Carles, N. Saint-Cricq, A. Zwick, M. A. Renucci, and J. B. Renucci, in *Proceedings of the International Conference on Phonon Physics (Bloomington, Indiana, 1981)* [J. Phys. (Paris) Colloq. **42**, C6-105 (1981)].
[14]N. P. Kekelidze, G. P. Kekelidze, and Z. D. Makharadze, J. Phys. Chem. Solids **34** 2117 (1973).
[15]For example, see D. N. Talwar and Bal. K. Agrawal, Phys. Rev. B **12**, 1432 (1975).
[16]E. Bedel, R. Carles, A. Zwick, and J. B. Renucci (unpublished).
[17]E. Jahne, Phys. Status Solidi B **75**, 221 (1976).
[18]R. Carles, N. Saint-Cricq, J. B. Renucci, A. Zwick, and M. A. Renucci, Phys. Rev. B **22**, 6120 (1980).
[19]R. Loudon, Proc. R. Soc. London, Ser. A **275**, 218 (1963); Adv. Phys. **13**, 423 (1964).
[20]R. M. Martin and L. M. Falicov, in *Light Scattering in Solids*

I, Vol. 8 of *Topics in Applied Physics*, edited by M. Cardona (Springer, Berlin 1980), p. 79.
[21]R. Trommer and M. Cardona, Phys. Rev. B **17**, 1865 (1978).
[22]M. Balkanski, C. Hirlimann, and J. F. Morhange, in *Proceedings of the International Conference on Lattice Dynamics, Paris, 1977*, edited by M. Balkanski (Flammarion, Paris, 1978), p. 174.
[23]C. Hirlimann, thèse d'Etat, Université de Paris VI, 1981.
[24]R. Carles, J. B. Renucci, A. Zwick, and M. A. Renucci, in *Proceedings of the International Conference on Physics of Non-crystalline Solids (Montpellier, France, 1982)* [J. Phys. Colloq. **43**, C9-363 (1982)].
[25]P. J. Colwell and M. V. Klein, Solid State Commun. **8**, 2095 (1970).
[26]S. Buchner, L. Y. Ching, and E. Burstein, Phys. Rev. B **14**, 4459 (1976).
[27]M. Zigone, R. Beserman, and M. Balkanski, in *Proceedings of the International Conference on Light Scattering in Solids, Paris, 1971*, edited by M. Balkanski (Flammarion, Paris, 1971), p. 61.
[28]P. Yu, H. Pilkuhn, and F. Evangelisti, Solid State Commun. **25**, 371 (1978).
[29]R. Carles, N. Saint-Cricq, A. Zwick, M. A. Renucci, and J. B. Renucci, in *Proceedings of the Vth International Conference on Ternary and Multinary Compounds, Cagliari, Italy, 1982* [Il Nuovo Cimento **2D**, 1712 (1983)].